

Downstream Flood Inundation Assessment due to Dam Breach of Dudh Koshi Storage Hydroelectric Project using HEC-RAS 2D

Biken Shrestha¹, Mukesh Raj Kafle¹, and Santosh Bhattarai¹

¹ Department of Civil Engineering, Pulchowk Campus, Institute of Engineering, Tribhuvan University, Nepal

Corresponding author: Biken Shrestha (078mshpe005.biken@pcampus.edu.np)

Key Points:

- Dam breach is catastrophic event in which peak breach discharge and flood arrival time is influenced by dam height.
- Overtopping failure mode is critical than piping mode of failure.
- Dam breach width is most sensitive parameter for overtopping and piping failure modes under local and global sensitivity analysis.

Abstract

Dam breach is rare event in which dam fails releasing impounded water to downstream regions. Dam breach has low probability of occurrence but carries high risk of destruction. Dudhkoshi Storage Hydroelectric Project concrete faced rock fill dam (CFRD) was studied for dam breach under overtopping and piping failure modes. Dam breach simulation and flood propagation study is vital for identifying and minimizing the risks associated with breach flood. Two scenarios namely base-case scenario with average value of dam breach parameters and worst-case scenario with value of dam breach parameters resulting in maximum output. Local and global sensitivity analysis are performed for four dam breach parameters (dam breach width, breach formation time, weir coefficient, trigger failure elevation). Sensitivity analysis is performed for two river profile. Sensitivity on peak discharge, peak velocity, arrival time and water surface elevation were evaluated. ArcGIS, HEC-RAS and OriginPro 2022b are used for dam breach analysis. Overtopping failure was found to be critical as compared to piping mode.

Plain Language Summary

The collapse of Dudh Koshi Hydroelectric Project dam will generate flood waves immediately destroying settlements near and beyond the dam site. The flood will travel along the river stream and sideways across river banks. The change in value of geometry and time associated with dam collapse changes the intensity of flood and arrival time of flood downstream. The depth of flood, arrival time of flood are mapped in terms of buildings, roads and local level affected downstream of dam.

1 Introduction

Dam breach is catastrophic failure which releases impounded water to immediate downstream resulting in loss of life and property. The causes of dam failure are earthquake, land slide, extreme precipitation, piping, equipment malfunctioning, structure damage, foundation failure and sabotage (Xiong, 2011; Brunner 2014). Vajont dam failed due to landslide (Barla & Paronuzzi, 2013), Kakhovka dam failed during Russia–Ukraine War (Vyshnevskyi et al., 2023)

39 and Shibuya dam failed due of underestimation of geotechnical parameter (Chrzanowski et al.,
40 2008). Banqiao Dam and the Shi-mantan Dam failure claimed the lives of around 85,000 (Sachin.,
41 2014). Concrete faced rock fill dam (CFRD) has been subjected to failure due to overtopping and
42 seepage erosion (Wahl, 1998; Xu & Zhang, 2009; Zhang et al., 2016). Various dam failures are
43 documented in literature. Gouhou (Zhang & Cheng, 2006), Zipingpu (Zou et al., 2013), Campos
44 Novos (Nieto, 2021), Aguamilpa (Ma & Cao, 2007), Tianshengqiao-1 (Ma & Chi, 2016) details
45 about mode and mechanisms of CFRD dam failure. CFRD failure occurs due to crack formation
46 which develops percolation channel along dam section (Zhang et al., 2016; Ma & Chi, 2016). The
47 impacts of dam failure can be controlled by using accurate flood hazard maps (Balaji & Kumar,
48 2018). (Mudashiru et al., 2021) reviewed flood hazard mapping for physical-based, empirical and
49 physical modelling. HEC-RAS is used for physical-based modelling.

50 (Eldeeb et al 2023) performed unsteady flow 2D dynamic routing and breach parameter
51 sensitivity analysis for Grand Ethiopian renaissance dam (GERD). (Kiwanka et al.,2023)
52 performed dam breach analysis of Kibimba dam under overtopping and piping mode of failure
53 with probable maximum flood as input. The breach parameters and the peak flow discharges were
54 calculated using the Froehlich, (1995) and Froehlich, (2008) regression equations. (Beza et al.,
55 2023; Khosravi et al., 2019; Sharma et al., 2017) used HEC-RAS for flood routing, flood plain
56 delineation and hazard mapping. (Karki et al., 2022, Gaagai et al., 2022) conducted sensitivity
57 analysis on dam breach parameters. Dam breach width, breach formation time, weir coefficient
58 piping coefficient, breach bottom elevation, side slope are considered for the dam breach study
59 (Brunner, 2014). (Ramola et al., 2021) modelled catchment area as storage area, flood hazard area
60 as 2D flow area and dam as SA/2D connection in HEC-RAS for Baur Dam in which overtopping
61 failure was found to be more critical than piping failure. (Albu et al., 2020) stated that dam breach
62 simulation can be validated through literature review. Dam breach model could perform without
63 manning's n calibration. (Bharath et al., 2021; Hicks & Peacock, 2005). (Psomiadis et al.,2021;
64 Phyou et al., 2023) compared overtopping and piping failure modes for dam breach analysis.
65 (Delenne et al., 2012) stated that sensitivity analysis can be used for shallow water equation
66 analysis in place of global sensitivity analysis with short computation time. Global sensitivity
67 analysis is critical for non-linear distribution (Iooss et al., 2015; Bellos et al., 2020).

68 Dudh Koshi Storage project lies on moderate seismic risk zone along active fault line
69 between Okhaldhunga and Khotang district of Nepal (Japan International Cooperation Agency
70 (JICA), 2014). Dudh Koshi basin has total glacierized area of approximately 410 km² of which
71 110 km² is debris covered (Shea et al., 2015). There is possibility of GLOF induced dam breach.
72 High intensity rainfall on 5-13 July, 2004 had activated landslides and debris flow in the watershed
73 of the Dudh Koshi River (Dhital, 2006). Storage project provides power system flexibility.
74 Dudhkoshi, Adhikhola, Sunkoshi 3, Upper Mustang, Bharbhung storage projects are under
75 different stages of study and development (NEA Annual Report, 2023). Storage HPP impound
76 large volume of water in steep topography and fragile geology with potential seismic risk. Dam
77 breach analysis should be performed for risk management. The objectives of this paper are:

- 78 (1) To determine dam breach outflow hydrograph for overtopping and piping failure at
79 dam site and river sections downstream of dam.
- 80 (2) To delineate dam breach flood hazard map for overtopping and piping failure.
- 81 (3) To perform sensitivity analysis of dam breach parameters to breach discharge, water
82 surface elevation, velocity and arrival time.

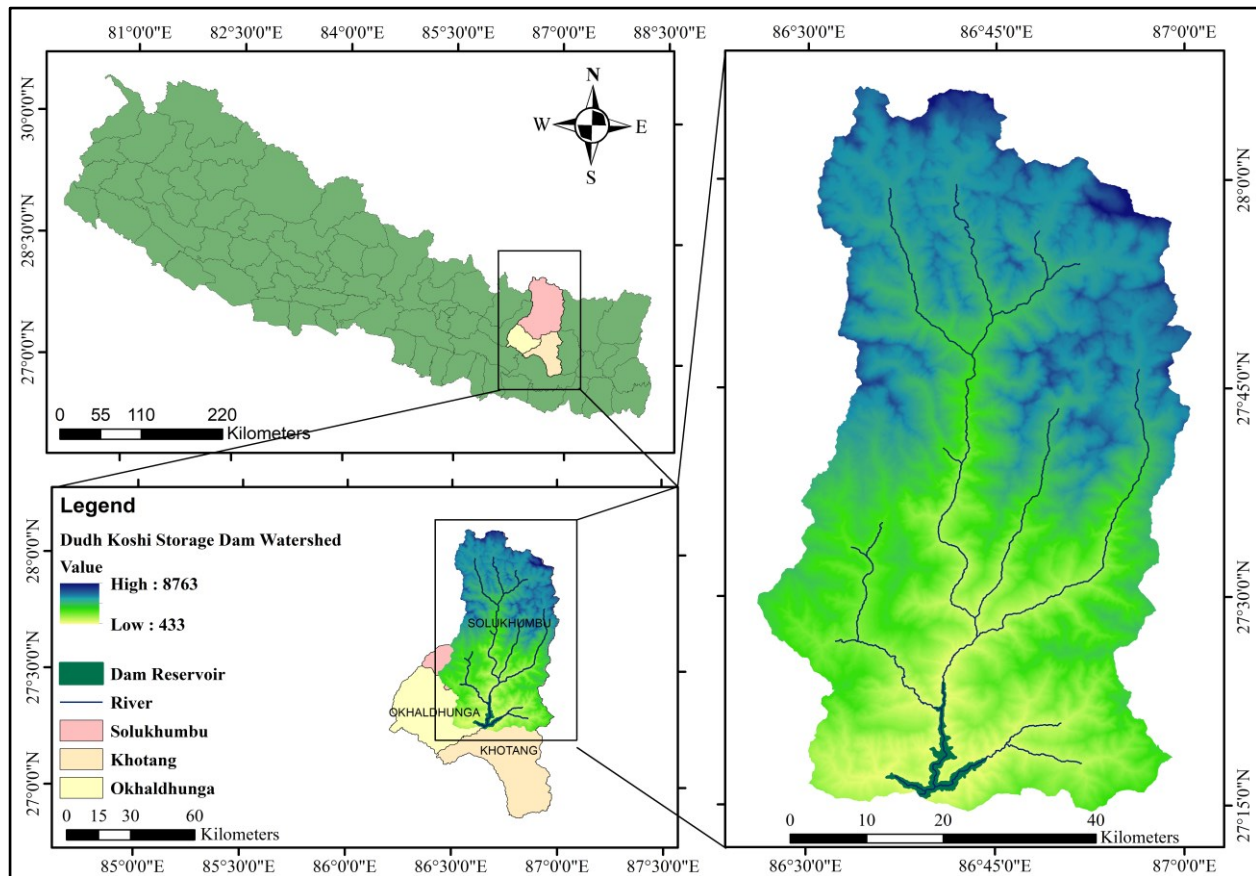
83 **2 Study Area and Data**84 **2.1 Study Area**

Figure 1: Study Area Map

85 The proposed Dudh Koshi storage hydroelectric project (DKSHEP) is a storage type
 86 project. The study area of DKSHEP is shown in Figure 1. The dam is located in the Dudh Koshi
 87 river approximately in the latitude of $27^{\circ} 15' 47''$ and longitude of $86^{\circ} 38' 17''$ which is about 2km
 88 downstream from the confluence of Thotne river and Dudh Koshi. DKSHEP dam is of concrete
 89 faced rockfill dam (CFRD) with crest length of 620m, crest width of 16m and height of 210m. The
 90 full supply level (FSL) is at 636 masl while the dam crest is at 640 masl. The catchment area of
 91 dam is 3851.89 km² while the capacity of reservoir is 1491.92 Mm³. Gated spillway and labyrinth
 92 spillway are present on left embankment of dam (Updated Feasibility Report of Dudh Koshi
 93 Storage Hydroelectric Project, 2019).

94 **2.2 Data Acquisition**

95 The reliability of dam breach modelling results depends upon DEM data. ALOS PALSAR,
 96 ASTER GDEM, Sentinel and AW3D30 DEM data were evaluated (Okolie and Smith, 2022).
 97 AW3D30 showed most accurate representation of river profile and adjusted to dam geometrical
 98 characteristic among DEM's considered. Rainfall data were analyzed using Thiessen polygon
 99 method to find mean annual rainfall. Shakya method (Shakya, 2002) was used to distribute the
 100 10000-year rainfall into 24-hour time domain which was multiplied with unit hydrograph ordinate
 101 obtained from Taylor's and Schwartz method (Taylor and Schwarz, 1952) to define the inflow

102 hydrograph for HEC-RAS analysis. 10,000-year flood hydrograph with peak discharge of 12638
 103 m³/s was used as inflow for HEC-RAS dam breach unsteady flow analysis. The shapefile for
 104 buildings and roads in study area is extracted from Geofabrik Open street map while population
 105 data is obtained from National Statistics Office, Nepal Census 2021. The source of data used for
 106 the research work is listed in Table 1.

107 Table 1

108 *Data Collection*

| Data | Source |
|-------------------------------|---|
| Digital Elevation Model (DEM) | 30m DEM from Japan Aerospace Exploration Agency (JAXA) Advanced Land Observing Satellite World 3D (AW3D30) https://www.eorc.jaxa.jp/ALOS/en/dataset/aw3d30 |
| Dam geometry | Dudh Koshi Storage Hydroelectric Project: Final upgraded feasibility study rev. 01 executive summary, 2019 |
| Precipitation | Department of Hydrology and Meteorology (DHM), Nepal: 1202, 1203, 1204, 1206, 1207, 1219, 1222, 1224, 1324 EVK2CNR: Everest Pyramid, Pheriche and Namche http://geonetwork.evk2cnr.org/ |
| Dam location | Contour of dam crest level, length of dam and dam geographic coordinates |
| Catchment area | Arc GIS |
| Buildings, Roads Shapefile | Geofabrik Open Street Map data |
| Land use | Sentinel 2 |
| Population | National Statistics Office, Population Census 2021 |

109 **3 Materials and Methods**

110 3.1 Methodology

111 The methodology used for dam breach analysis of Dudh Koshi Hydroelectric Project
 112 (DKSHEP) dam is shown in Figure 2. The result of dam breach analysis is fully dependent upon
 113 selection of breach parameter. Federal agency guidelines from USACE 1980; USACE 2007;
 114 FERC; NWS (Brunner, 2014), regression equation based on dam failure dataset (Froehlich, 1995a;
 115 Froehlich, 2008; MacDonald and Langdridge-Monopolis 1984; Von Thun and Gillete, 1990; Xu
 116 and Zhang, 2009), simplified breach model, physically based breached model are used for
 117 estimation of dam breach parameters. The dam breach parameters are selected on the basis of
 118 USACE, 2007 federal guidelines as Froehlich equation and other empirical equation are derived
 119 for dam of height upto 92m (Brunner, 2014).

120 The catchment area of Dudh Koshi Storage hydroelectric project (DKSHEP) dam was
 121 delineated in ArcGIS and modelled as storage area in HEC-RAS. The flood hazard area was
 122 modelled as 2D flow area. Dam geometry was modelled as SA/2D connection in HEC- RAS RAS
 123 mapper (Brunner, 2014). Downstream outlet was fixed at Koshi barrage while backwater effect
 124 was observed upto Likhu - Sunkoshi confluence. Labyrinth spillway was modelled for overtopping
 125 failure while gated spillway is assumed to be closed. The piping failure case was modelled without
 126 spillway for model simplicity and stability. Cell size of 40 m* 40m with break line of 40 m spacing
 127 to align cells along river profile was used for simulation.

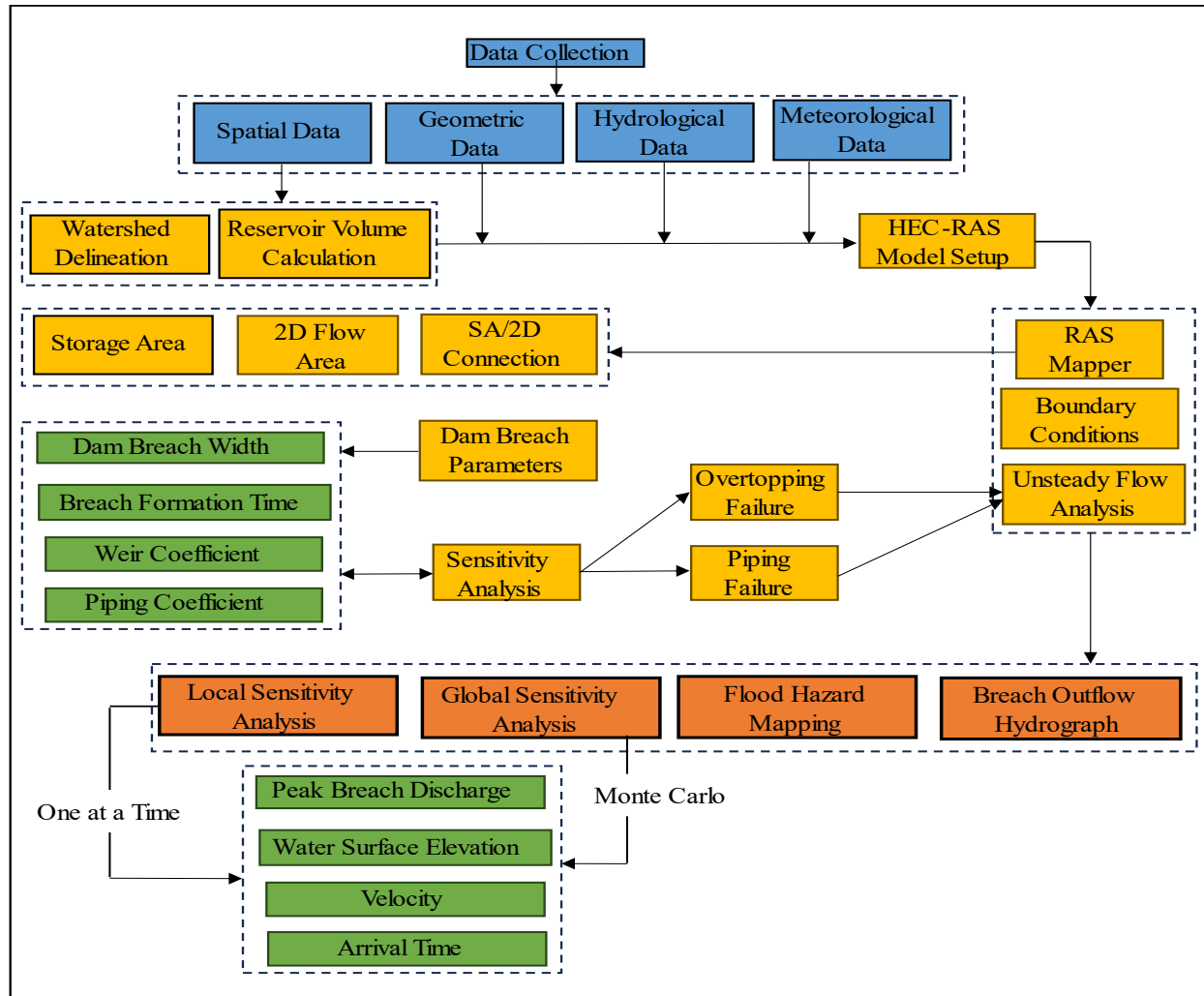


Figure 2: *Flowchart of methodology used for dam breach analysis*

128 Overtopping failure mode was simulated with fixed time step of 3 seconds while courant
 129 condition was used for piping failure. Shallow Water Equation (SWE) was used for accurate
 130 representation of velocity as compared to diffusion wave equation (Brunner, 2014). Pilot model
 131 run showed diffusion peak velocity three times of velocity obtained from SWE for overtopping
 132 failure. Five dam breach parameters were considered for sensitivity analysis. Dam breach width,
 133 breach formation time, weir coefficient, trigger failure elevation was used for overtopping failure
 134 while piping coefficient was used instead of trigger failure elevation for piping failure. The shallow
 135 water equation used for dam breach analysis is shown in Equation 1), Equation 2) and Equation
 136 3). The full supply level is considered as initial water level during HEC-RAS analysis.
 137 Overtopping failure only occurs when the water level rises above dam crest whereas piping failure
 138 occurs through pipe channel formation in dam section (Chen et al., 2019).

139

140

141

142 **Continuity Equation**

$$\left(\frac{\partial H}{\partial t}\right) + \frac{\partial(hu)}{\partial x} + \frac{\partial(hv)}{\partial y} = 0 \quad \text{Equation 1}$$

143 **Momentum Equation in X - Direction**

$$\left(\frac{\partial u}{\partial t}\right) + u \left(\frac{\partial u}{\partial x}\right) + v \left(\frac{\partial u}{\partial y}\right) + g \left(\frac{\partial H}{\partial x}\right) + u \left(\frac{gn^2|u|}{R^{4/3}}\right) = 0 \quad \text{Equation 2}$$

144 **Momentum Equation in Y - Direction**

$$\left(\frac{\partial v}{\partial t}\right) + u \left(\frac{\partial v}{\partial x}\right) + v \left(\frac{\partial v}{\partial y}\right) + g \left(\frac{\partial H}{\partial y}\right) + v \left(\frac{gn^2|v|}{R^{4/3}}\right) = 0 \quad \text{Equation 3}$$

145 Where, H is water surface elevation (m), h is water depth, u and v are depth averaged
 146 velocities in x and y direction (m/s), g is acceleration due to gravity (m/s²), n is manning's
 147 coefficient and R is wetted perimeter (m).

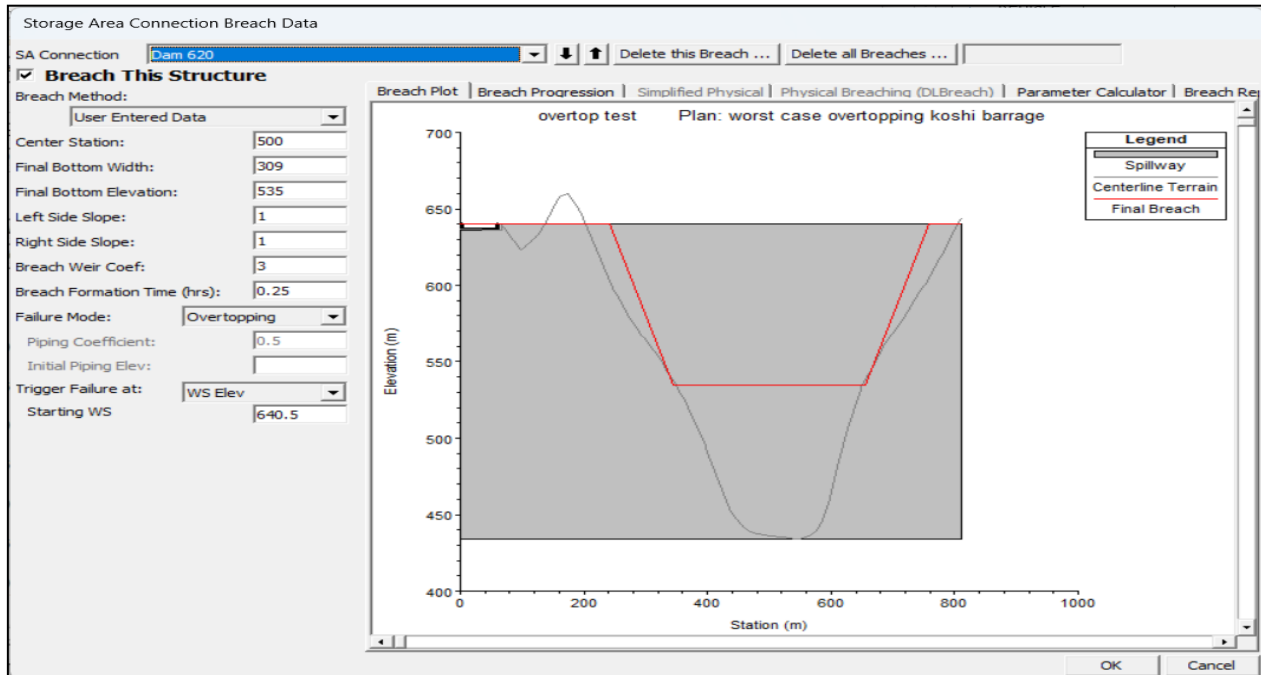


Figure 3: *Worst Case Dam Breach Cross Section for Overtopping Failure*

148 The worst-case scenario with worst combination of dam breach parameter was provided
 149 for dam breach analysis flood hazard mapping. The HEC-RAS dam breach data interface, dam
 150 cross section and labyrinth spillway geometry is shown in Figure 3 with input value for
 151 overtopping failure worst case scenario. Sensitivity Analysis (SA) is a method for studying model
 152 reliability and robustness. It is used to identify the influential parameters and quantify their impact
 153 on model outcomes (Saltelli et al., 2004). Monte Carlo filtering is used for local calibration of data
 154 set in sensitivity analysis (Saltelli, 2002). Different types, methods and procedures for sensitivity
 155 analysis are found in the literature (Saltelli et al., 2021; Ghanem et al., 2017; Iooss et al., 2015; D.G.
 156 Cacuci & Ionescu-Bujor, 2005; Frey & Patil, 2002). Local sensitivity analysis (LSA) determines

157 the local influence of input factor variation on the model response (Zhou & Lin, 2008). OAT
 158 methods are adequate for linearly varying models while non-linear models with high parameter
 159 uncertainty must be analyzed using GSA (Saltelli et al., 2019). (Iooss et al., 2015) presents different
 160 methods for global sensitivity analysis. Pseudo global sensitivity with standard deviation-based
 161 Monte Carlo simulation was used for the research work (Karki et al., 2022). 3*3*3*3 matrix of
 162 four dam breach parameter with three cases will be used to create 81 permutation plans.

163 4 Results

164 4.1. Breach Flood Hydrograph

165 The dam breach analysis was conducted for both overtopping and piping failure modes.
 166 Headwater stage hydrograph and tailwater stage hydrograph for overtopping failure are shown in
 167 Figure 4 and Figure 5 while breach discharge hydrograph and velocity hydrograph for overtopping
 168 failure at dam location are shown in Figure 6 and Figure 7 respectively.

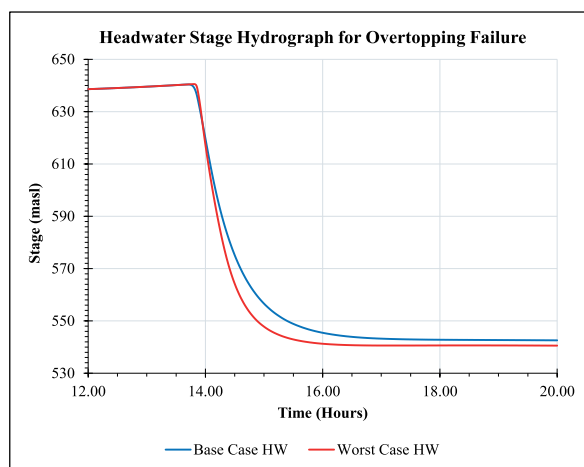


Figure 4: *Headwater Stage Hydrograph for overtopping failure*

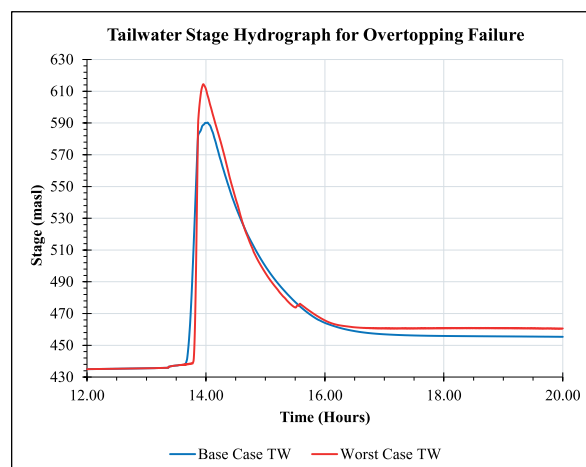


Figure 5: *Tailwater Stage Hydrograph for overtopping failure*

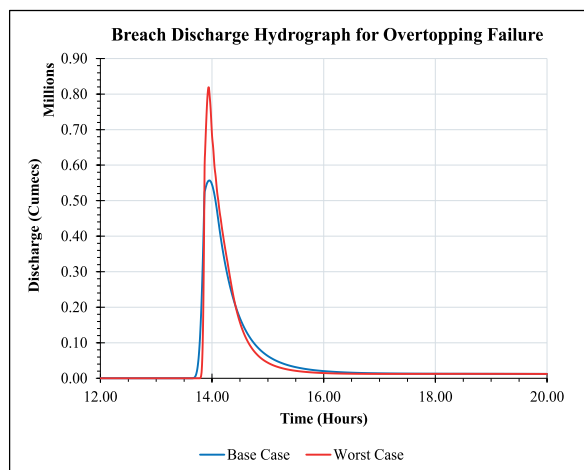


Figure 6: *Breach discharge Hydrograph for overtopping failure*

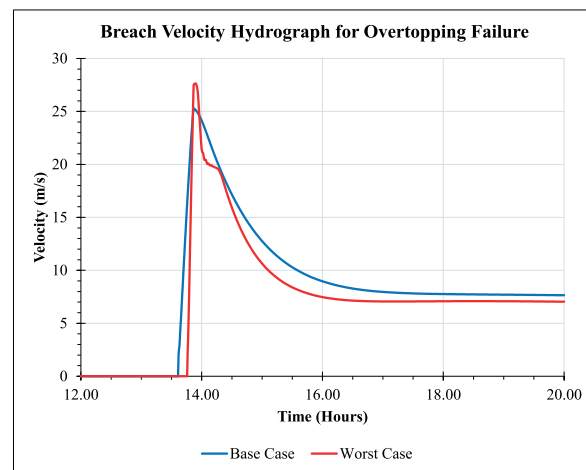


Figure 7: *Breach velocity Hydrograph for overtopping failure*

169 The flooded area from overtopping failure is only slightly greater than that of piping failure
 170 while discharge and velocity for worst case is greater than that for base case scenario as seen in
 171 Table 2.

172 Table 2

173 *Dam Breach flood Hydrograph*

| Description | Overtopping Failure | | Piping Failure | |
|------------------------|-----------------------------|-----------------------------|-----------------------------|-----------------------------|
| | Base Case | Worst Case | Base Case | Worst Case |
| Flooding Area | 72.27 km ² | 72.31 km ² | 67.94 km ² | 69.62 km ² |
| Peak Discharge | 556710.69 m ³ /s | 817456.80 m ³ /s | 491115.50 m ³ /s | 753351.60 m ³ /s |
| Time of Peak Discharge | 13:57:30 PM | 13:56:30 PM | 00:24:30 AM | 00:11:30 AM |
| Peak Velocity | 25.29 m/s | 27.63 m/s | 27.63 m/s | 29.90 m/s |
| Time of Peak Velocity | 13:52:00 PM | 13:53:30 PM | 00:15:00 AM | 00:06:00 AM |

174 *Note.* Base case represents average values of breach parameters while worst case represented worst
 175 combination of breach parameters. Time of Peak discharge and velocity is represented from start
 176 of simulation at 00:00:00 rather than start of breach.

177 4.2. Breach Flood Routing

178 The discharge was routed along R1 and R2 profile for base case and worst-case scenario
 179 under overtopping and piping failure case. R1 profile represents river profile from dam location to
 180 Sunkoshi bridge outlet located 85km downstream of dam while R2 profile represents river profile
 181 from Dudhkoshi-Sunkoshi confluence to Likhu-Sunkoshi confluence.

182 Table 3

183 *Flood Routing for Overtopping Failure*

| Scenario | River Profile | Overtopping Failure | | | | | |
|------------|---------------|------------------------------------|-----------|----------|----------------------|----------|----------|
| | | Peak Discharge [m ³ /s] | | | Arrival Time [hours] | | |
| | R1 | 0.25 km | 30 km | Outlet | 0.25 km | 30 km | Outlet |
| | R2 | 1 km | 10 km | | 1 km | 10 km | |
| Base Case | R1 | 554440.56 | 114739.37 | 76899.48 | 13:57:30 | 15:08:00 | 18:17:30 |
| | R2 | 25539.50 | 12627.43 | 125.26 | 16:49:30 | 16:32:00 | 16:37:00 |
| Worst Case | R1 | 810742.25 | 122779.41 | 78648.09 | 13:56:00 | 14:59:30 | 18:11:00 |
| | R2 | 27790.88 | 13941.19 | 219.67 | 16:40:00 | 16:46:00 | 16:33:00 |

184

185 Table 4

186 *Flood Routing for Piping Failure*

| Scenario | River Profile | Piping Failure | | | | | |
|------------|---------------|------------------------------------|-----------|----------|----------------------|---------|---------|
| | | Peak Discharge [m ³ /s] | | | Arrival Time [hours] | | |
| | R1 | 0.25 km | 30 km | Outlet | 0.25 km | 30 km | Outlet |
| | R2 | 1 km | 10 km | | 1 km | 10 km | |
| Base Case | R1 | 488484.22 | 104858.06 | 68847.26 | 0:24:30 | 1:34:30 | 4:43:00 |
| | R2 | 23207.53 | 11508.02 | 887.76 | 3:10:00 | 3:01:00 | 3:00:30 |
| Worst Case | R1 | 748480.56 | 113088.15 | 70680.77 | 0:12:00 | 1:17:00 | 4:26:00 |
| | R2 | 25606.30 | 12910.41 | 11.25 | 2:47:30 | 2:42:00 | 2:47:30 |

187 *Note:* The flood routing for R1 profile is done from dam location to Sunkoshi bridge outlet while
 188 for R2 profile the routing is done from Dudhkoshi – Sunkoshi confluence upto Likhu – Sunkoshi
 189 confluence. The distance value represents river section for R1 and R2 profile respectively. The
 190 arrival time is calculated from start of simulation.

191 The peak discharge for flood routing is shown in Table 3 for overtopping failure and Table
 192 4 for piping failure. The breach occurs immediately after simulation for piping failure as trigger
 193 elevation is set at initial water level. Overtopping failure only occurs when the water level rises
 194 from full supply level to crest level and finally to overtopping trigger elevation with labyrinth
 195 spillway operational. The overtopping occurs nearly 13.5 hours after start of simulation. There is
 196 sudden drop in peak at 30km downstream of dam this is due to dispersion of water in Dudhkoshi
 197 - Sunkoshi confluence and backwater flow towards Likhu-Sunkoshi confluence. The peak
 198 discharge flood routing showed that overtopping failure discharge has higher peak and longer
 199 arrival time as compared to piping failure. The worst and base case scenario for both failure modes
 200 showed varying behavior in terms of discharge at the start of breach while on downstream end the
 201 flood showed similar nature for both scenarios.

202 4.3. Flood Inundation and Hazard Mapping

203 Dam breach flood hazard mapping was performed in terms of depth, velocity, arrival time
 204 and water surface elevation with Koshi barrage as outlet. (Mudashiru, 2021) reviewed the use of
 205 HEC-RAS for flood hazard mapping. The number of local levels affected, number of buildings
 206 and length of road network for overtopping and piping failure modes are shown in Table
 207 5. Population at risk (PAR) due to overtopping dam breach failure is 1,34,211 while PAR due to
 208 piping failure of Dudh Koshi Storage Hydroelectric Project dam is at 1,21,437.

Table 5

Dam breach flood Hydrograph

| Parameters | Overtopping Failure | Piping Failure |
|-------------|---|---|
| Local Level | 12 municipality | 12 municipality |
| | 20 rural municipality | 21 rural municipality |
| | Koshi Tappu Wildlife Reserve in 3 districts | Koshi Tappu Wildlife Reserve in 3 districts |
| Buildings | 28,032 | 25,343 |
| Roads | 812.35 km | 776.87 km |
| PAR | 1,34,211 | 1,21,437 |

209 The locality near dam site will be completely destroyed by dam breach in matter of seconds
 210 as peak discharge associated with breach is in the range of 0.75 to 0.87 million cubic meter for
 211 piping and overtopping failures. The depth of flood reduces along downstream river profile. Water
 212 depth is high along narrow river reach while it reduces sideways about the floodplain. The sudden
 213 change in depth profile 30km downstream of dam location is due to dispersion of flow along
 214 Dudhkoshi - Sunkoshi confluence. The velocity is critical near dam location due to high head
 215 associated with overtopping failure.

216 The inundation mapping shows that Dudh Koshi storage hydroelectric project (DKSHEP)
 217 dam breach flood will travel along the river profile until the Dudh Koshi - Sunkoshi confluence,
 218 The breach flood will then disperse along Sunkoshi River. Part of flow will move downstream

219 towards Sunkoshi powerhouse tailrace location while another part will backflow upstream towards
 220 Likhu – Sunkoshi confluence. The downstream flow will again dissipate along Arun and Tamor
 221 confluence at Tribeni before finally moving to Koshi barrage through Chatara. The flood
 222 inundation plain due to dam breach under worst case scenario of overtopping failure is shown in
 223 Figure 8 and Figure 9 for R1 and R2 profile respectively.

224 The flood hazard mapping of depth, velocity, arrival time and water surface elevation is
 225 shown in Table 6.

Table 6
 Flood Inundation and Hazard Mapping

| Description | Overtopping Failure | Piping Failure | River Profile |
|----------------|-----------------------------|-----------------------------|---------------|
| Peak Discharge | 866229.40 m ³ /s | 753341.30 m ³ /s | |
| Flooding Area | 686.29 km ² | 670.62 km ² | |
| Depth | 0 m - 181 m | 0 m - 177 m | R1 |
| | 0 m - 80 m | 0 m - 78 m | R2 |
| Velocity | 0 m/s - 45 m/s | 0 m/s - 41 m/s | R1 |
| | 0 m/s - 24 m/s | 0 m/s - 22 m/s | R2 |
| WSE | 75 m - 640.5 m | 74 m - 620 m | R1 |
| | 400 m - 431 m | 400 m - 424 m | R2 |
| Arrival Time | 13 hrs - 32 hrs | 0 hrs - 20 hrs | R1 |
| | 15 hrs - 17 hrs | 1 hrs - 3 hrs | R2 |

226

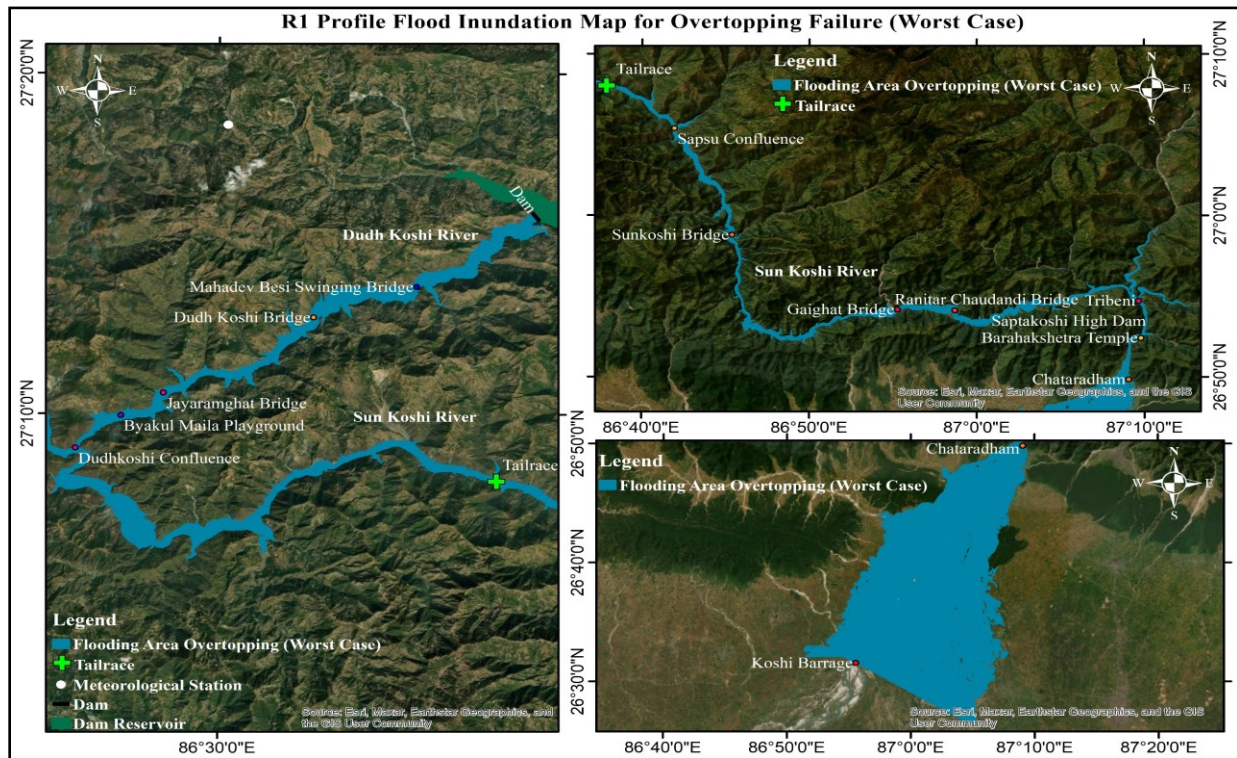


Figure 8: Overtopping Flood Inundation Mapping for R1 Profile

227

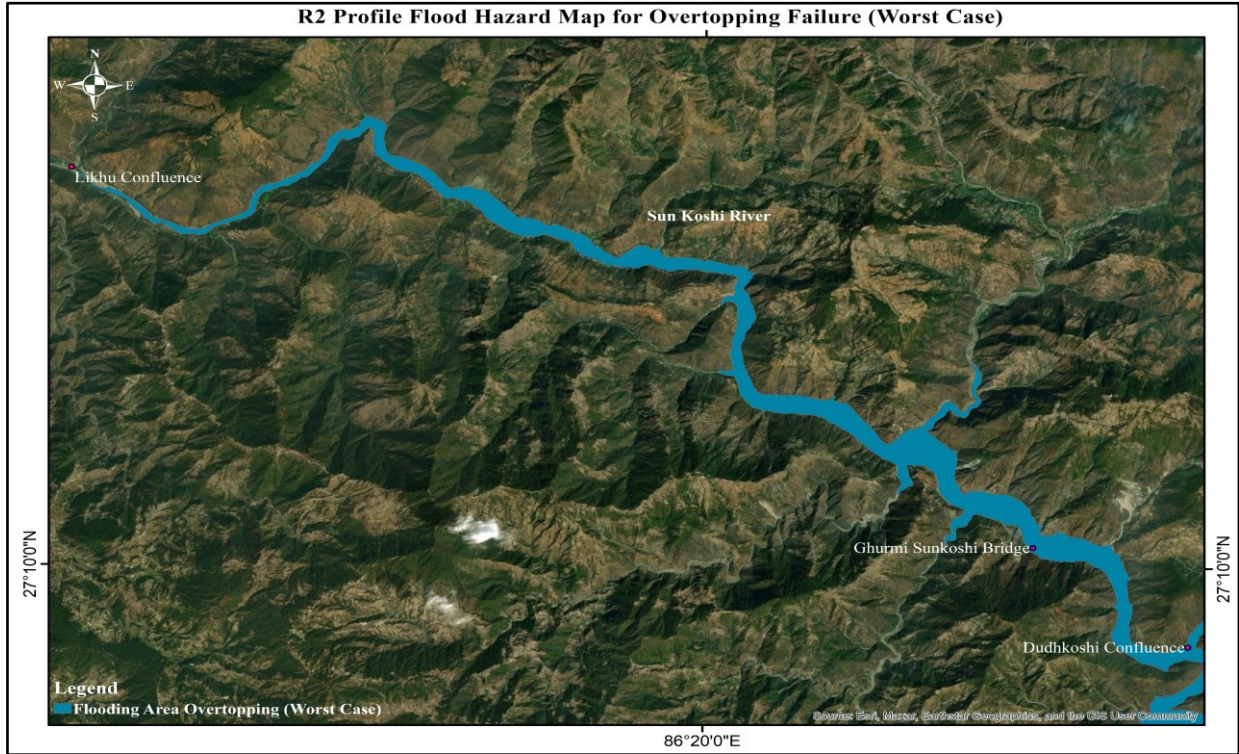


Figure 9: *Overtopping Flood Inundation Mapping for R2 Profile*

228 The overtopping failure depth mapping for R1 profile is shown in Figure 10 which
 229 represents maximum breach flood depth of 112m at Mahadev besi swinging bridge, 106m at
 230 Jayaramghat bridge, 75 m at Dudh Koshi - Sunkoshi confluence, 50 m near the tailrace, 47 m at
 231 Tribeni, 40 m at proposed Saptakoshi high dam and 2 m at Koshi barrage outlet.

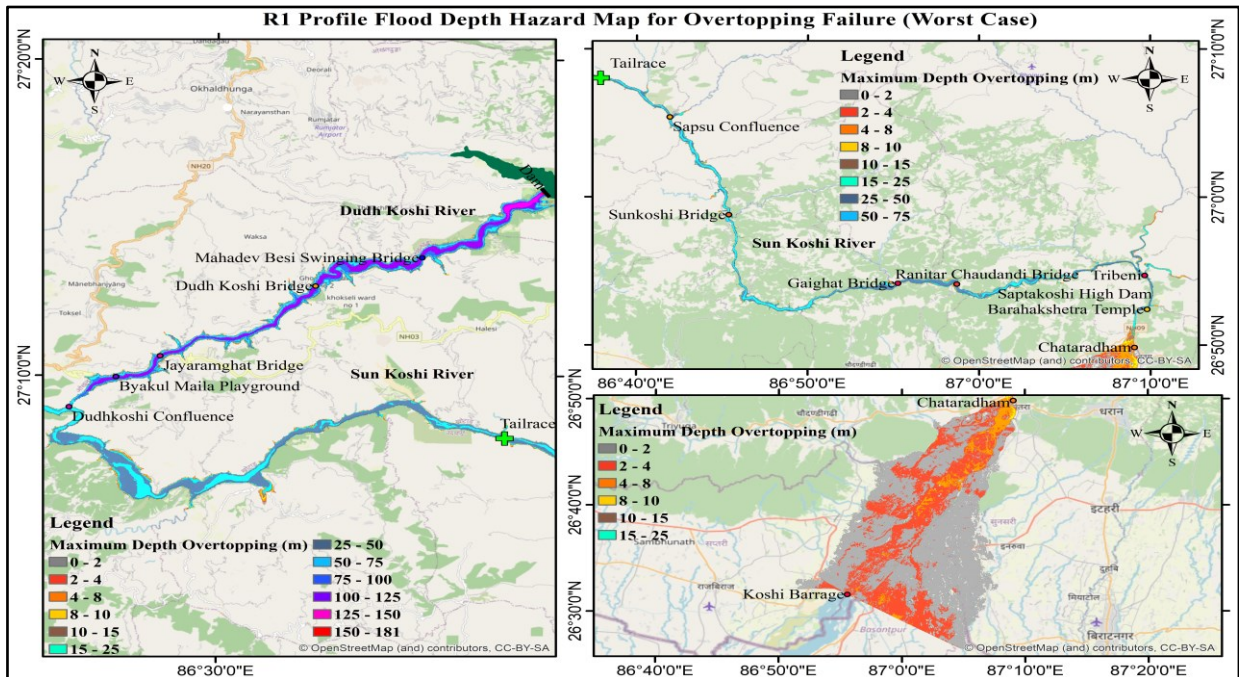


Figure 10: *Overtopping Flood Depth Mapping for R1 Profile*

232 The depth mapping for R2 profile is shown in Figure 11 which represents flood depth of
 233 53 m at Ghurmi Sunkoshi bridge and 0.02m near Likhu - Sunkoshi confluence.

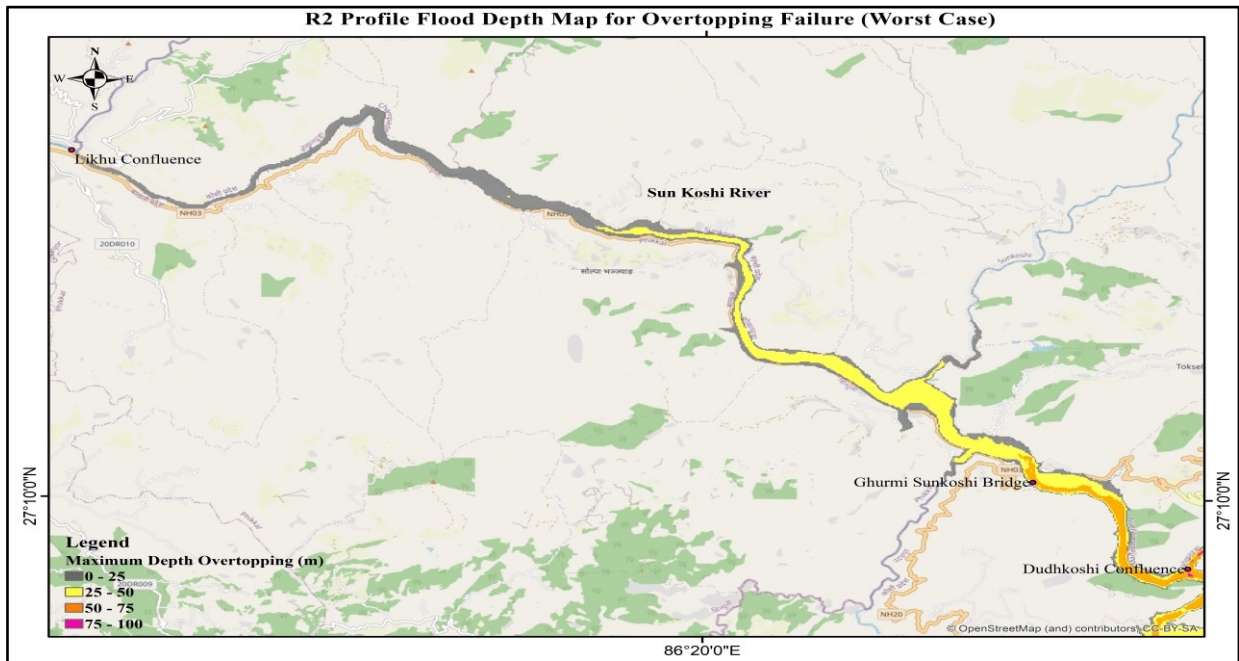


Figure 11: Overtopping Flood Depth Mapping for R2 Profile

234 The maximum velocity at Mahadev besi swinging bridge, Jayaramghat bridge, Dudh Koshi
 235 - Sunkoshi confluence, tailrace is 25m/s, 14m/s, 23m/s, 10m/s respectively while maximum
 236 velocity is 5 m/s at Tribeni, 11 m/s at proposed Saptakoshi high dam and 4 m/s Koshi barrage
 237 outlet for R1 profile as shown in Figure 12.

238

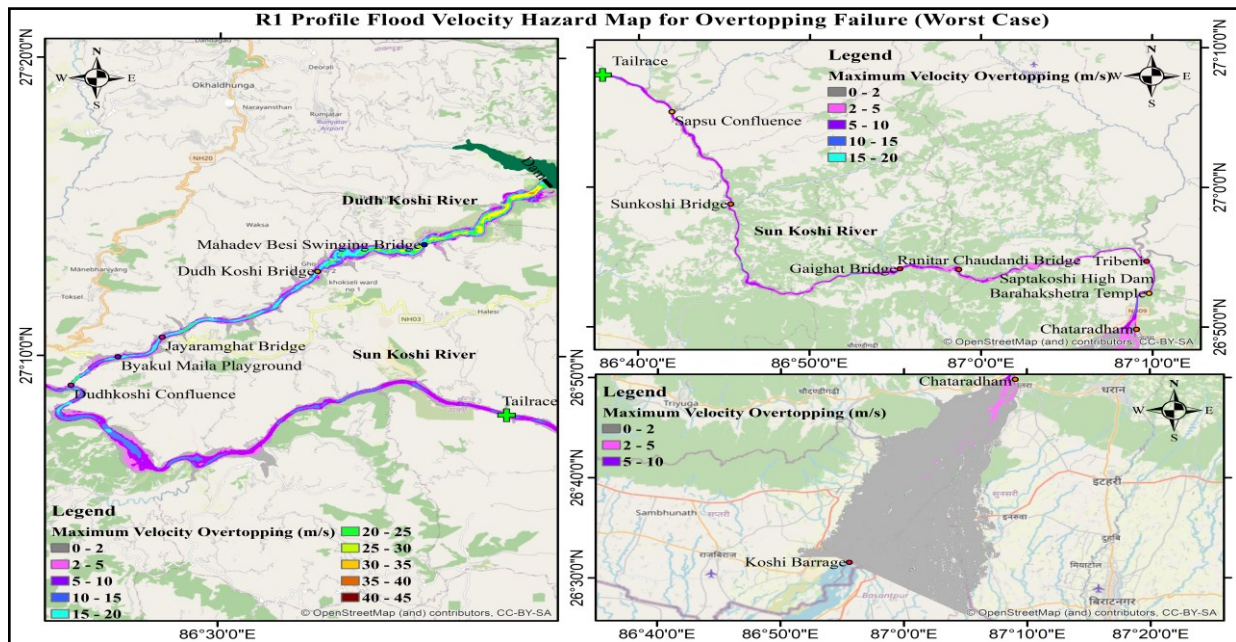


Figure 12: Overtopping Flood Velocity Mapping for R1 Profile

239 The velocity mapping for R2 profile depicts 10m/s at Ghurmi Sunkoshi bridge and 0.2 near
 240 Likhu - Sunkoshi confluence as shown in Figure 13.

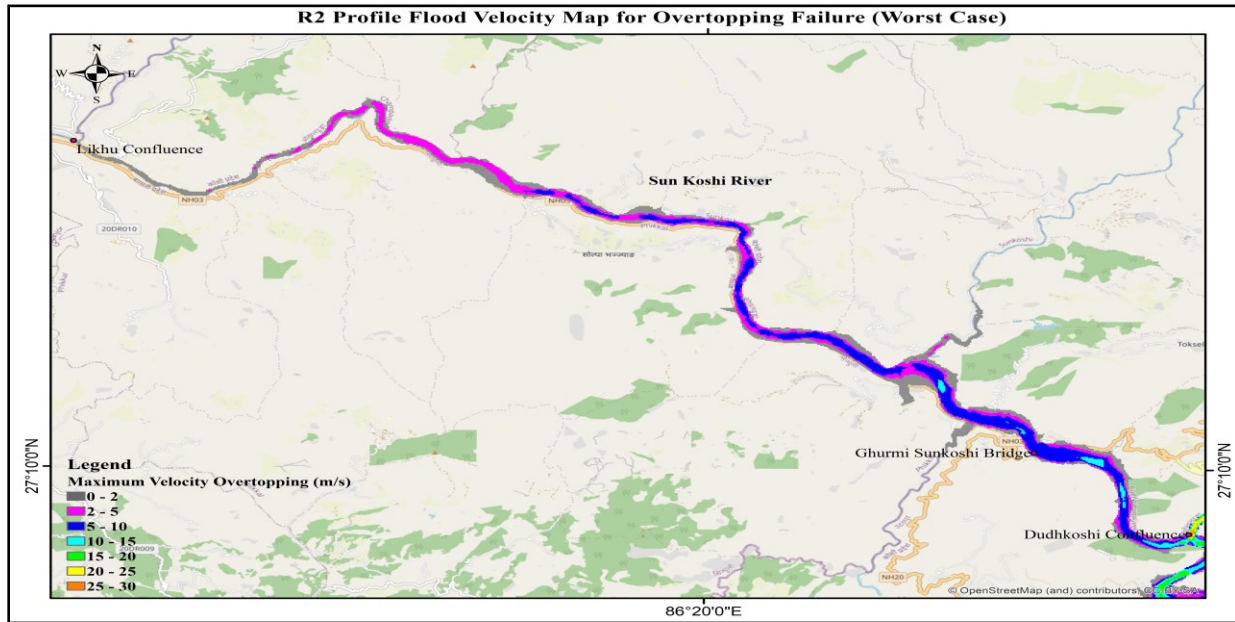
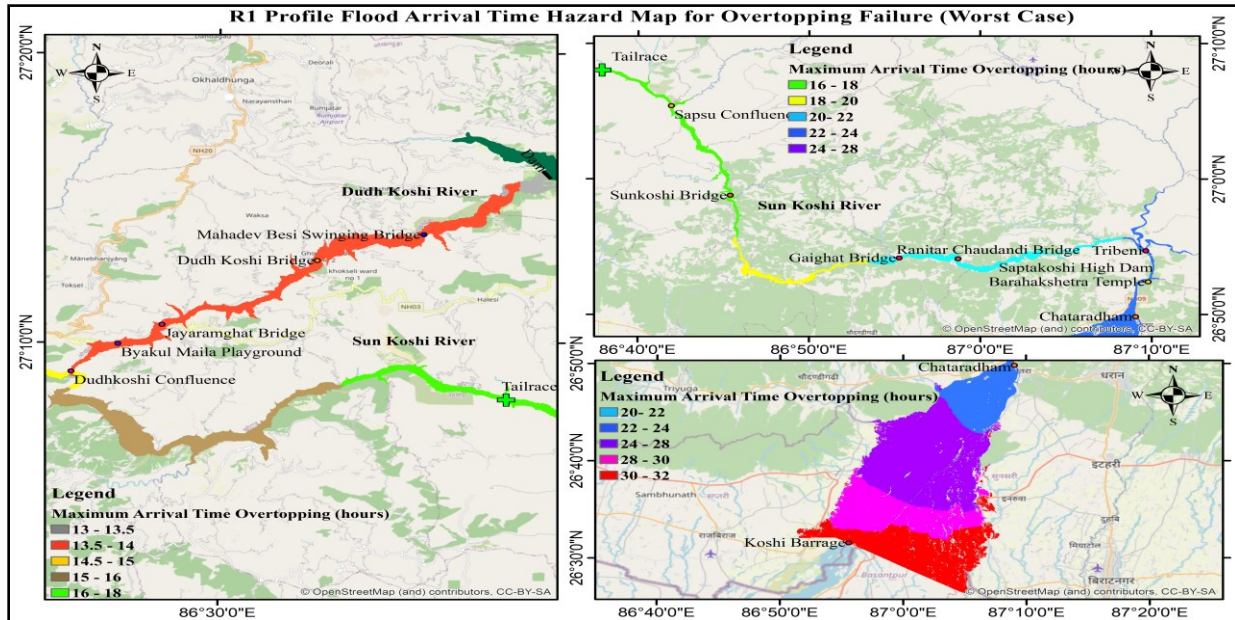


Figure 13: Overtopping Flood Velocity Mapping for R2 Profile

241 The maximum arrival time for breach flood is 14.3 hours at Mahadev besi swinging bridge,
 242 14.8 hours at Jayaramghat bridge, 15.5 hours at Dudh Koshi – Sunkoshi confluence, 17.4 hours at
 243 tailrace, 23.4 hours at Tribeni, 23.5 hours at proposed Saptakoshi high dam and 32 hours at Koshi
 244 barrage location for R1 profile as shown in Figure 14.

245

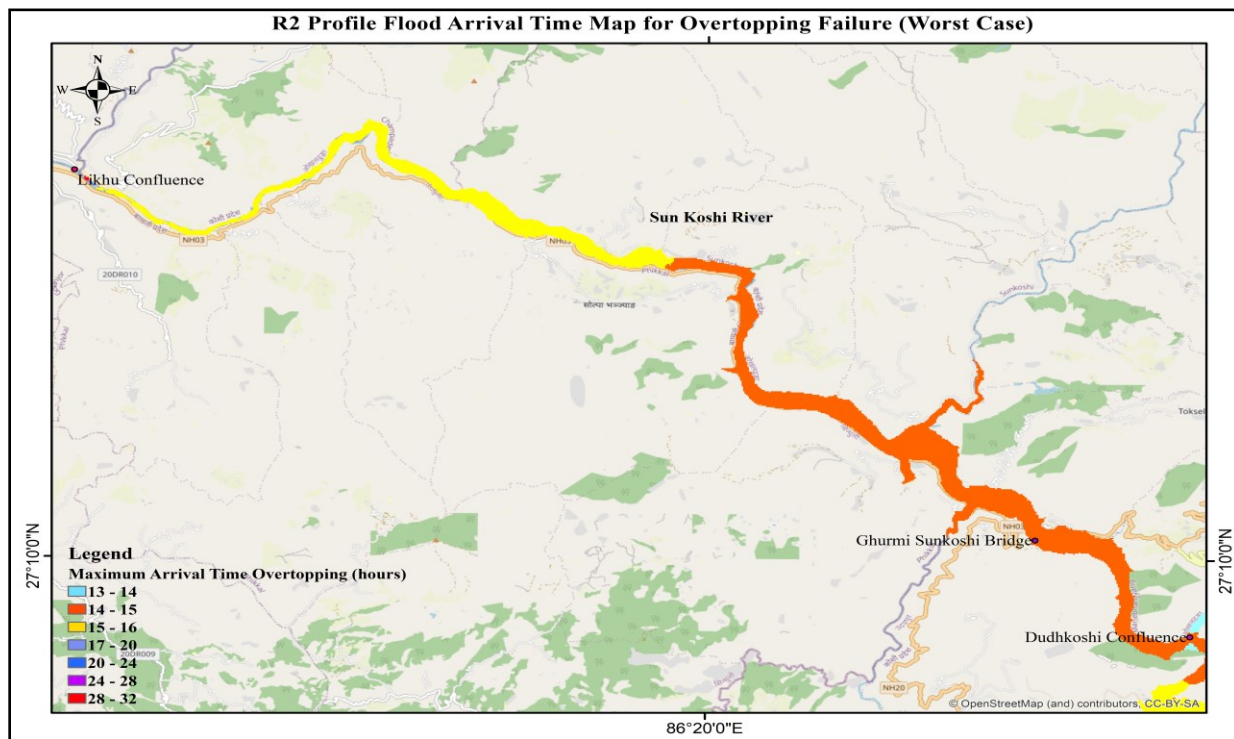


246

247

Figure 14: Overtopping Flood Arrival Time Mapping for R1 Profile

248 The maximum arrival time for R2 profile the maximum arrival time is 15.5 hours for Ghurmi
 249 Sunkoshi bridge and 16.5 hours near Likhu - Sunkoshi confluence as shown in Figure 14 and
 250 Figure 15 respectively.
 251



252
 253 *Figure 15: Overtopping Flood Arrival Time Mapping for R2 Profile*

254 4.4. Sensitivity Analysis

255 4.4.1. Local Sensitivity Analysis

256 Local sensitivity analysis was performed using one at a time (OAT) approach. Dam breach
 257 parameters were ranked on the basis of ratio of percentage change in output per unit percentage
 258 change in input. Trigger failure elevation is most sensitive and breach formation time is least
 259 sensitive for local sensitivity analysis of peak discharge for overtopping failure while for piping
 260 failure weir coefficient is most sensitive parameters and piping coefficient is least sensitive as
 261 shown in Table 7 and Table 8. The research results shows that trigger elevation defines the peak
 262 discharge, water surface elevation, velocity and arrival time downstream of dam after breach for
 263 overtopping failure while weir coefficient is driving factor for piping failure mode for downstream
 264 impacts under local sensitivity analysis.

Table 7
Local sensitivity analysis for overtopping failure

| Sensitivity on | Overtopping Failure | | Weir Coefficient | Trigger Elevation |
|-------------------|---------------------|-----------------------|------------------|-------------------|
| | Dam Breach Width | Breach Formation Time | | |
| Peak Discharge | 0.3657 | 0.2784 | 0.7171 | 10.5255 |
| WSE (R1) | 0.0530 | 0.0182 | 0.0785 | 1.5329 |
| WSE (R2) | 0.0102 | 0.0004 | 0.0106 | 0.0059 |
| Velocity (R1) | 0.1085 | 0.0838 | 0.1636 | 0.2420 |
| Velocity (R2) | 0.1666 | 0.0016 | 0.1923 | 0.0469 |
| Arrival Time (R1) | 0.0262 | 0.0131 | 0.0275 | 0.1276 |
| Arrival Time (R2) | 0.0245 | 0.0148 | 0.0286 | 0.2158 |

Table 8
Local sensitivity analysis for piping failure

| Sensitivity on | Piping Failure | | Weir Coefficient | Piping Coefficient |
|-------------------|------------------|-----------------------|------------------|--------------------|
| | Dam Breach Width | Breach Formation Time | | |
| Peak Discharge | 0.4720 | 0.3186 | 0.7275 | 0.0284 |
| WSE (R1) | 0.0644 | 0.0185 | 0.0794 | 0.0365 |
| WSE (R2) | 0.0113 | 0.0003 | 0.0125 | 0.0027 |
| Velocity (R1) | 0.1068 | 0.1314 | 0.1928 | 0.1183 |
| Velocity (R2) | 0.2198 | 0.0373 | 0.2511 | 0.0429 |
| Arrival Time (R1) | 0.1179 | 0.0617 | 0.1228 | 0.0645 |
| Arrival Time (R2) | 0.1766 | 0.1115 | 0.1700 | 0.0170 |

265 4.4.2. Global Sensitivity Analysis

266 Five lakh sample data within permutation range was used for Monte Carlo simulation with
 267 Monte Carlo filtering for outputs results in Origin Pro. Global sensitivity analysis was examined
 268 on the basis of variation of standard deviation of outputs with respect to variation of standard
 269 deviation of inputs. Dam breach width is most sensitive parameter followed by breach formation
 270 time. weir coefficient and trigger failure elevation for global sensitivity analysis of peak discharge
 271 for overtopping failure while for piping failure dam breach width is most sensitive parameter
 272 followed by breach formation time. weir coefficient and piping coefficient as shown in **Error!**
 273 **Reference source not found.** and **Error! Reference source not found.** The research result shows
 274 that dam breach width is most sensitive parameter for both
 275 overtopping and piping failure hence the width of breach will mainly define the downstream
 276 impacts from the breach under global sensitivity analysis of dam breach parameters

277

278

279

280

281

282

Table 9
Global Sensitivity Analysis for Overtopping Failure

| Sensitivity on | Overtopping Failure | | | |
|----------------|---------------------|-----------------------|------------------|-------------------|
| | Dam Breach Width | Breach Formation Time | Weir Coefficient | Trigger Elevation |
| Peak Discharge | 46350.57 | 44264.01 | 5214.57 | 468.85 |
| Peak Velocity | 0.1186 | 0.0993 | 1.2735 | 0.0026 |
| WSE | 0.5993 | 0.0038 | 0.0153 | 0.0081 |
| Arrival Time | 0.1727 | 0.0388 | 0.0036 | 0.0590 |

Table 10
Global Sensitivity Analysis for Piping Failure

| Sensitivity on | Piping Failure | | | |
|----------------|------------------|-----------------------|------------------|--------------------|
| | Dam Breach Width | Breach Formation Time | Weir Coefficient | Piping Coefficient |
| Peak Discharge | 96195.07 | 31808.50 | 4259.15 | 291.53 |
| Peak Velocity | 0.0188 | 0.0114 | 1.4303 | 0.0128 |
| WSE | 0.8137 | 0.0019 | 0.0126 | 0.0017 |
| Arrival Time | 0.1933 | 0.0541 | 0.0025 | 0.0005 |

283

284

285 6 Discussions

286 The dam breach analysis of Dudh Koshi storage hydroelectric project (DKSHEP) was
 287 performed for overtopping and piping modes of failure under worst case and base case scenario.
 288 The results obtained from analysis are summarized as follows:

- 289 (1) Overtopping failure was found to be critical mode of dam breach failure for peak
 290 discharge and flood plain area while piping failure mode was critical for arrival time.
 291 The outflow hydrograph for worst case scenario showed greater discharge, larger flood
 292 plain, higher velocity profile and faster arrival time as compared to base case scenario
 293 for both overtopping and piping failure modes.
- 294 (2) The peak discharge flood routing showed that overtopping failure discharge have
 295 higher peak and longer arrival time as compared to piping failure. The worst and base
 296 case scenario for both failure modes showed varying behavior in terms of discharge at
 297 the start of breach while on downstream end the flood showed similar nature for both
 298 scenarios.
- 299 (3) The flood routing for proposed Saptakoshi High dam located 143 km downstream of
 300 DKSHEP dam location showed peak depth at 40.87 m, peak discharge of 48163.65
 301 m³/s with arrival time at 23.44 hours from start of simulation and 9.67 hours after start
 302 of breach. The maximum velocity of dam breach flood is 11 m/s with WSE of 158.86
 303 m for overtopping failure under worst case scenario.

- 304 (4) Flood hazard mapping for worst case scenario was performed for Koshi barrage outlet.
305 Peak discharge and flood plain area of overtopping failure was critical. The variation
306 of depth, velocity, arrival time and water surface elevation were studied.
- 307 (5) 12 municipality, 20 rural municipality and Koshi Tappu Wildlife Reserve in 3 districts
308 would be affected with 28,032 buildings and 812.35 km of road under dam breach flood
309 risk for overtopping failure. The population at risk is 1,34,211.
- 310 (6) 12 municipality, 21 rural municipality and Koshi Tappu Wildlife Reserve in 3 districts
311 will be affected with 25,343 buildings and 776.87 km of road under dam breach flood
312 risk for piping failure. The population at risk is 1,21,437.

313 **7 Conclusions**

- 314 (1) The breach outflow hydrograph for overtopping and piping failure was determined for
315 base case and worst-case scenario while flood routing was performed up to Sunkoshi
316 bridge outlet.
- 317 (2) Flood hazard mapping was performed with respect to depth, velocity, arrival time and
318 water surface elevation at Koshi barrage outlet for worst case scenario under
319 overtopping and piping failure modes. The local levels affected, population at risk of
320 hazard, buildings and roads flooded due to dam breach hazard was determined.
- 321 (3) Trigger failure elevation was most sensitive parameter for overtopping scenario and
322 weir coefficient was most sensitive parameter for piping scenario under local sensitivity
323 analysis while for global sensitivity analysis dam breach width was most sensitive for
324 both overtopping and piping failure scenario.
325

326 **8 Validation**

- 327 (1) Dam breach parameters were selected as per USACE (2007) guidelines.
- 328 (2) Dam breach bottom elevation was selected within dam cross section as per State of
329 Colorado Guidelines for Dam breach analysis (2020).
- 330 (3) (Mudashiru et al., 2021) reviewed flood hazard mapping methods which presented use
331 of HEC-RAS 2D model for dam breach flood hazard mapping.
- 332 (4) (Psomiadis et al., 2021; Phyou, 2023) concluded that flooded area for overtopping
333 scenario is slightly larger than piping scenario in case of DEM data which aligns with
334 research work.
- 335 (5) (Abdulrazzaq et al., 2021) sensitivity analysis for Hamrin Dam showed that increase in
336 DBW increased the peak discharge while increase in BFT decreased the peak
337 discharge.
- 338 (6) (Karki et al., 2022) dam breach analysis on Nalgad Hydroelectric Project depicted WC
339 parameter as more sensitive than DBW and BFT for Peak Discharge and WSE while
340 for arrival time, TFE was most sensitive parameter which aligned with result obtained
341 for R1 profile in LSA while for GSA on peak discharge and WSE, DBW was found
342 most sensitive parameter.
343

344 9 Limitations

- 345 (1) Dam breach flood hazard mapping was done for Koshi barrage outlet while local
 346 sensitivity analysis, global sensitivity analysis and downstream flood routing was done
 347 for Sunkoshi bridge outlet lying 85 km downstream of dam location.
- 348 (2) Dam breach bottom elevation was fixed to 535masl due to cross sectional constraint
 349 for both overtopping and piping failure analysis. Gated spillway is assumed to be closed
 350 for overtopping failure analysis.
- 351 (3) Only four dam breach parameters were considered for sensitivity analysis.

352 Acknowledgements

353 I would like to thank all the esteemed faculty members of Department of Civil
 354 Engineering, Pulchowk Campus for the guidance throughout the study. I am thankful to
 355 Bashanta Dhoj Shrestha for providing 'Final upgraded feasibility study rev.01 Executive
 356 Summary' dated March, 2019 that was required for the study.

357 Open Research

359 Rainfall data processing was done in excel (Mohanty et al.,2014). Buildings and road
 360 shapefile was obtained from geofabric open street map (Singla et al., 2021). Dam breach analysis
 361 was performed in HEC RAS 6.4 (Brunner,2014). Flood hazard mapping was performed in
 362 ArcGIS 10.8.3 (Negesse et al., 2022). Origin Pro 2022 was used for global sensitivity analysis of
 363 dam breach parameters (Karki et al., 2022).

364 References

- 366 Abdulrazzaq, I. D., Jalut, Q. H., & Abbas, J. M. (2021). Sensitivity analysis for dam breach
 367 parameters using different approaches for earth-fill dam. *Diyala Journal of Engineering*
 368 *Sciences*, 14(4), 90-97. <https://doi.org/10.24237/djes.2021.14408>
- 369 Albu, L.-M., Enea, A., Iosub, M., & Breabăn, I.-G. (2020). Dam Breach Size Comparison for
 370 Flood Simulations. A HEC-RAS Based, GIS Approach for Drăcșani Lake, Sitna River,
 371 Romania. *Water*, 12(4). <https://doi.org/10.3390/w12041090>
- 372 Authority, N. E. (2023). *Annual Report 2023*.
 373 https://nea.org.np/admin/assets/uploads/supportive_docs/NEA_Annual_Report_2023.pdf
- 374 Balaji, B., & Kumar, S. (2018). Dam break analysis of Kalyani dam using HEC-RAS.
 375 *International Journal of Civil Engineering and Technology*, 9.
- 376 Barla, G., & Paronuzzi, P. (2013). The 1963 Vajont Landslide: 50th Anniversary. *Rock Mechanics*
 377 *and Rock Engineering*, 46(6), 1267-1270. <https://doi.org/10.1007/s00603-013-0483-7>
- 378 Bellos, V., Tsakiris, V. K., Kopsiaftis, G., & Tsakiris, G. (2020). Propagating Dam Breach
 379 Parametric Uncertainty in a River Reach Using the HEC-RAS Software. *Hydrology*, 7(4),
 380 72-72. <https://doi.org/10.3390/hydrology7040072>
- 381 Beza, M., Fikre, A., Moshe, A., & Vignali, V. (2023). Dam Breach Modeling and Downstream
 382 Flood Inundation Mapping Using HEC-RAS Model on the Proposed Gumara Dam,

- 383 Ethiopia. *Advances in Civil Engineering*, 2023, 1-15.
384 <https://doi.org/10.1155/2023/8864328>
- 385 Bharath, A., Shivapur, A. V., Hiremath, C. G., & Maddamsetty, R. (2021). Dam break analysis
386 using HEC-RAS and HEC-GeoRAS: A case study of Hidkal dam, Karnataka state, India.
387 *Environmental Challenges*, 5, 100401-100401.
388 <https://doi.org/10.1016/j.envc.2021.100401>
- 389 Brunner, G. W. (2014). Using HEC-RAS for Dam Break Studies.
390 <https://www.hec.usace.army.mil/publications/TrainingDocuments/TD-39.pdf>
- 391 Brunner, G. W. (2023). *HEC-RAS 2D User's Manual*.
- 392 Cacuci, D. G., Ionescu-Bujor, M., & Navon, I. M. (2005). Sensitivity and uncertainty analysis:
393 Applications to large-scale systems.
394 <https://doi.org/10.1201/9780203483572>
- 395 Chen, S.-s., Zhong, Q.-m., & Shen, G.-z. (2019). Numerical modeling of earthen dam breach due
396 to piping failure. *Water Science and Engineering*, 12(3), 169-178.
397 <https://doi.org/10.1016/j.wse.2019.08.001>
- 398 Delenne, C., Cappelaere, B., & Guinot, V. (2012). Uncertainty analysis of river flooding and dam
399 failure risks using local sensitivity computations. *Reliability Engineering & System Safety*,
400 107, 171-183. <https://doi.org/10.1016/j.res.2012.04.007>
- 401 Derdous, O., Djemili, L., Bouchehed, H., & Tachi, S. E. (2015). A GIS based approach for the
402 prediction of the dam break flood hazard – A case study of Zardezas reservoir “Skikda,
403 Algeria”. *Journal of Water and Land Development*, 27(1), 15-20.
404 <https://doi.org/10.1515/jwld-2015-0020>
- 405 Dhital, M. R. (2006). Impact of July 2004 high-intensity rain on Hilepani-Jayaramghat-Diktel
406 Environment-Friendly Road in East Nepal. *Journal of Nepal Geological Society*, 34, 81-
407 94. <https://doi.org/10.3126/jngs.v34i0.31882>
- 408 Eldeeb, H., Mowafy, M. H., Salem, M. N., & Ibrahim, A. (2023). Flood propagation modeling:
409 Case study the Grand Ethiopian Renaissance dam failure. *Alexandria Engineering Journal*,
410 71, 227-237. <https://doi.org/10.1016/j.aej.2023.03.054>
- 411 Frey, H. C., & Patil, S. R. (2002). Identification and review of sensitivity analysis methods. *Risk*
412 *Analysis*, 22(3), 553-578. <https://doi.org/10.1111/0272-4332.00039>
- 413 Froehlich, D. C. (1995). Embankment dam breach parameters revisited. International Water
414 Resources Engineering Conference - Proceedings,
- 415 Froehlich, D. C. (2008). Embankment Dam Breach Parameters and Their Uncertainties. *Journal*
416 *of Hydraulic Engineering*, 134(12), 1708-1721. [https://doi.org/10.1061/\(asce\)0733-9429\(2008\)134:12\(1708\)](https://doi.org/10.1061/(asce)0733-9429(2008)134:12(1708))
- 417
- 418 Gaagai, A., Aouissi, H. A., Krauklis, A. E., Burlakovs, J., Athamena, A., Zekker, I., Boudoukha,
419 A., Benaabidate, L., & Chenchouni, H. (2022). Modeling and Risk Analysis of Dam-Break
420 Flooding in a Semi-Arid Montane Watershed: A Case Study of the Yabous Dam,
421 Northeastern Algeria. *Water*, 14(5). <https://doi.org/10.3390/w14050767>
- 422 Ghanem, R., Higdon, D., & Owhadi, H. (2017). Handbook of Uncertainty Quantification.
423 <https://doi.org/10.1007/978-3-319-12385-1>
- 424 Hicks, F. E., & Peacock, T. (2005). Suitability of HEC-RAS for Flood Forecasting. *Canadian*
425 *Water Resources Journal*, 30(2), 159-174. <https://doi.org/10.4296/cwrj3002159>
- 426 Iooss, B., & Lemaître, P. (2015). A review on global sensitivity analysis methods. *Operations*
427 *Research/ Computer Science Interfaces Series*, 59. https://doi.org/10.1007/978-1-4899-7547-8_5
- 428

- 429 JICA. (2014). *Nationwide Master Plan Study on Storage-type Hydroelectric Power Development*
430 *in Nepal*.
- 431 Karki, A., Bhattarai, S., Joshi, P., Kafle, M., & Bhattarai, R. (2022). Dam Breach Analysis and
432 Parameter Sensitivity Analysis Along a River Reach Using Hecras. *Stavebni obzor - Civil*
433 *Engineering Journal*, 31(4), 571-585. <https://doi.org/10.14311/cej.2022.04.0043>
- 434 Khosravi, K., Rostamnejad, M., Cooper, J. R., Mao, L., & Melesse, A. M. (2019). Dam break
435 analysis and flood inundation mapping: The case study of Sefid-Roud Dam, Iran. In
436 *Extreme Hydrology and Climate Variability* (pp. 395-405). [https://doi.org/10.1016/b978-](https://doi.org/10.1016/b978-0-12-815998-9.00031-2)
437 [0-12-815998-9.00031-2](https://doi.org/10.1016/b978-0-12-815998-9.00031-2)
- 438 Kiwanuka, M., Chelangat, C., Mubialiwo, A., Lay, F. J., Mugisha, A., Mbujje, W. J., & Mutanda,
439 H. E. (2023). Dam breach analysis of Kibimba Dam in Uganda using HEC-RAS and HEC-
440 GeoRAS. *Environmental Systems Research*, 12(1). [https://doi.org/10.1186/s40068-023-](https://doi.org/10.1186/s40068-023-00317-4)
441 [00317-4](https://doi.org/10.1186/s40068-023-00317-4)
- 442 Ma, H., & Cao, K. (2007). Key technical problems of extra-high concrete faced rock-fill dam.
443 *Science in China Series E: Technological Sciences*, 50(S1), 20-33.
444 <https://doi.org/10.1007/s11431-007-6007-5>
- 445 Ma, H., & Chi, F. (2016). Technical Progress on Researches for the Safety of High Concrete-Faced
446 Rockfill Dams. *Engineering*, 2(3), 332-339. <https://doi.org/10.1016/j.Eng.2016.03.010>
- 447 MacDonald, T. C., & Langridge-Monopolis, J. (1984). Breaching Characteristics of Dam Failures.
448 *Journal of Hydraulic Engineering*, 110(5), 567-586. [https://doi.org/10.1061/\(asce\)0733-](https://doi.org/10.1061/(asce)0733-9429(1984)110:5(567))
449 [9429\(1984\)110:5\(567\)](https://doi.org/10.1061/(asce)0733-9429(1984)110:5(567))
- 450 Mohanty, P. K., Panigrahi, D., & Acharya, M. (2014). MissRF: A Visual Basic Application in MS
451 Excel to Find out Missing Rainfall Data and Related Analysis. *Intelligent Information*
452 *Management*, 06(02), 38-44. <https://doi.org/10.4236/iim.2014.62006>
- 453 Mudashiru, R. B., Sabtu, N., Abustan, I., & Balogun, W. (2021). Flood hazard mapping methods:
454 A review. In *Journal of Hydrology* (Vol. 603).
- 455 Negese, A., Worku, D., Shitaye, A., & Getnet, H. (2022). Potential flood-prone area identification
456 and mapping using GIS-based multi-criteria decision-making and analytical hierarchy
457 process in Dega Damot district, northwestern Ethiopia. *Applied Water Science*, 12(12).
458 <https://doi.org/10.1007/s13201-022-01772-7>
- 459 Nieto, C. *Mechanical behavior of rockfill materials-Application to concrete face rockfill dams*
- 460 Okolie, C. J., & Smit, J. L. (2022). A systematic review and meta-analysis of Digital elevation
461 model (DEM) fusion: pre-processing, methods and applications. *ISPRS Journal of*
462 *Photogrammetry and Remote Sensing*, 188, 1-29.
463 <https://doi.org/10.1016/j.isprsjprs.2022.03.016>
- 464 Phyto, A. P., Yabar, H., & Richards, D. (2023). Managing dam breach and flood inundation by
465 HEC-RAS modeling and GIS mapping for disaster risk management. *Case Studies in*
466 *Chemical and Environmental Engineering*, 8. <https://doi.org/10.1016/j.cscee.2023.100487>
- 467 Psomiadis, E., Tomanis, L., Kavvadias, A., Soulis, K. X., Charizopoulos, N., & Michas, S. (2021).
468 Potential Dam Breach Analysis and Flood Wave Risk Assessment Using HEC-RAS and
469 Remote Sensing Data: A Multicriteria Approach. *Water*, 13(3).
470 <https://doi.org/10.3390/w13030364>
- 471 Ramola, M., Nayak, P. C., Basappa, V., & Thomas, T. (2021). Dam Break Analysis using HEC-
472 RAS and Flood Inundation Modelling for Pulichinatala Dam in Andhra Pradesh, India.
473 *Indian Journal of Ecology*, 48, 620-626.
- 474 Resources, S. o. C. D. o. N. (2020). *Guidelines for dam breach analysis*.

- 475 Saltelli, A. (2002). Sensitivity analysis for importance assessment. *Risk Analysis*,
476 Saltelli, A., Aleksankina, K., Becker, W., Fennell, P., Ferretti, F., Holst, N., Li, S., & Wu, Q.
477 (2019). Why so many published sensitivity analyses are false: A systematic review of
478 sensitivity analysis practices. *Environmental Modelling & Software*, 114, 29-39.
479 <https://doi.org/10.1016/j.envsoft.2019.01.012>
- 480 Saltelli, A., Jakeman, A., Razavi, S., & Wu, Q. (2021). Sensitivity analysis: A discipline coming
481 of age. *Environmental Modelling & Software*, 146.
482 <https://doi.org/10.1016/j.envsoft.2021.105226>
- 483 Saltelli, A., Ratto, M., Andres, T., Campolongo, F., Cariboni, J., Gatelli, D., Saisana, M., &
484 Tarantola, S. (2007). *Global Sensitivity Analysis. The Primer*. wiley.
485 <https://doi.org/10.1002/9780470725184>
- 486 Saltelli, A., Tarantola, S., Campolongo, F., & Ratto, M. (2004). *Sensitivity Analysis in Practice. A*
487 *Guide to Assessing Scientific Models*. In: *Probability and Statistics Series*.
- 488 Shakya, B. (2002). Guidelines for estimation of average rainfall depth of probable maximum
489 precipitation (PMP) over Bagmati basin of Nepal. XXI-
490 Conf Bucharest 2002 Proceedings,
- 491 Sharma, P. (2016). Dam Break Analysis Using HEC-RAS and HEC-GeoRAS – A Case Study of
492 Ajwa Reservoir. *Journal of Water Resources and Ocean Science*, 5(6), 108-108.
493 <https://doi.org/10.11648/j.wros.20160506.15>
- 494 Shea, J. M., Wagnon, P., Immerzeel, W. W., Biron, R., Brun, F., & Pellicciotti, F. (2015). A
495 comparative high-altitude meteorological analysis from three catchments in the Nepalese
496 Himalaya. *International Journal of Water Resources Development*, 31(2), 174-200.
497 <https://doi.org/10.1080/07900627.2015.1020417>
- 498 Singla, J. G., & Padia, K. (2020). A Novel Approach for Generation and Visualization of Virtual
499 3D City Model Using Open Source Libraries. *Journal of the Indian Society of Remote*
500 *Sensing*, 49(6), 1239-1244. <https://doi.org/10.1007/s12524-020-01191-8>
- 501 Snyder, F. F. (1938). Synthetic Unit-Graphs. *Transactions American Geophysics Union*, 19, 447-
502 454.
- 503 Taylor, A. B., & Schwarz, H. E. (2014). Unit-hydrograph lag and peak flow related to basin
504 characteristics. *Eos, Transactions American Geophysical Union*, 33(2), 235-246.
505 <https://doi.org/10.1029/TR033i002p00235>
- 506 USACE. (1980). *Flood Emergency Plans - Guidelines for Corps dams, RD-13*. Hydrological
507 Engineering Center.
- 508 Von Thun, J. L., & Gillette, D. R. (1990). Guidance on breach parameters. *US Department of the*
509 *Interior, Bureau of Reclamation*.
- 510 Vyshnevskiy, V., Shevchuk, S., Komorin, V., Oleynik, Y., & Gleick, P. (2023). The destruction
511 of the Kakhovka dam and its consequences. In *Water International* (Vol. 48).
- 512 Wahl, T. L. (1998). Prediction of Embankment Dam Breach Parameters: Literature Review and
513 Needs Assessment, Dam Safety Research Report. *U.S. Department of the Interior Bureau*
514 *of Reclamation Dam Safety Office*(July).
- 515 Wahl, T. L. (2004). Uncertainty of Predictions of Embankment Dam Breach Parameters. *Journal*
516 *of Hydraulic Engineering*, 130(5), 389-397. [https://doi.org/10.1061/\(asce\)0733-9429\(2004\)130:5\(389\)](https://doi.org/10.1061/(asce)0733-9429(2004)130:5(389))
- 517
518 Xiong, Y. (2011). A Dam Break Analysis Using HEC-RAS. *Journal of Water Resource and*
519 *Protection*, 03(06), 370-379. <https://doi.org/10.4236/jwarp.2011.36047>

- 520 Xu, Y., & Zhang, L. M. (2009). Breaching Parameters for Earth and Rockfill Dams. *Journal of*
521 *Geotechnical and Geoenvironmental Engineering*, 135(12), 1957-1970.
522 [https://doi.org/https://doi.org/10.1061/\(ASCE\)GT.1943-5606.000012](https://doi.org/10.1061/(ASCE)GT.1943-5606.000012)
- 523 Zhang, L., Peng, M., Chang, D., & Xu, Y. (2016). *Dam Failure Mechanisms and Risk Assessment*.
524 John Wiley & Sons. <https://doi.org/10.1002/9781118558522>
- 525 Zhang, L. M., & Chen, Q. (2006). Seepage Failure Mechanism of the Gouhou Rockfill Dam
526 During Reservoir Water Infiltration. *Soils and Foundations*, 46(5), 557-568.
527 <https://doi.org/10.3208/sandf.46.557>
- 528 Zhou, X., & Lin, H. (2017). *Local Sensitivity Analysis*. [https://doi.org/10.1007/978-3-319-17885-](https://doi.org/10.1007/978-3-319-17885-1_703)
529 [1_703](https://doi.org/10.1007/978-3-319-17885-1_703)
- 530 Zou, D., Xu, B., Kong, X., Liu, H., & Zhou, Y. (2013). Numerical simulation of the seismic
531 response of the Zipingpu concrete face rockfill dam during the Wenchuan earthquake based
532 on a generalized plasticity model. *Computers and Geotechnics*, 49, 111-122.
533 <https://doi.org/10.1016/j.compgeo.2012.10.010>
534